Mining, Metallurgy & Exploration (2020) 37:211–217
https://doi.org/10.1007/s42461-019-00123-6

Shielding Material Comparison for Electromagnetic Interference Mitigation for the Air Pump Motor of Personal Dust Monitors

Jingcheng Li[1] · Jacob Carr[1] · Cory DeGennaro[1] · Bruce Whisner[1] · Patrick McElhinney[1]

Received: 24 April 2019 / Accepted: 31 July 2019 / Published online: 16 August 2019

Abstract

Since 2016, electromagnetic interference (EMI) of personal dust monitors (PDMs) with magnetic proximity detection systems (PDSs) has been observed in underground coal mines. The EMI causes the magnetic field measurements of a PDS to change, which, in turn, alters the calculated location of the miner relative to the machine. Any altered location calculation can potentially cause the PDS to fail to warn a worker who is at an unsafe distance from the machine, arousing a serious concern on safety hazard caused by EMI in underground mines. The search for EMI mitigation strategies led to the development and use of large shielding pouches and boxes to hold the entire PDM to reduce its magnetic emission. Research on these pouches and boxes found that although they were able to reduce the emitted radiation from the PDM, they also disturbed the magnetic field of the PDS, affecting its performance. Researchers from the National Institute for Occupational Safety and Health (NIOSH) have focused on shielding internal PDM components rather than shielding the entire PDM. The PDM air pump motor is one of the PDM components that has been identified as a major source of electromagnetic radiation and has been selected for further study and tests. The measurements show that a small copper or aluminum foil enclosure can effectively reduce the magnetic emission of the motor by between 50 and 85% at 73 kHz. This study compares the test results of the air pump motor with various cost-effective shielding materials. The data provided in this paper can serve as a reference for shielding enclosure design of the PDM air pump motor to reduce its electromagnetic emission as one form of EMI mitigation strategy.

Keywords Electromagnetic interference · Electromagnetic shielding · Personal dust monitor · Proximity detection system

1 Introduction

Work in underground coal mines presents a number of uniquely difficult safety and health challenges. Among the health hazards is the risk of respiratory diseases due to dust exposure. To address this hazard, the Mine Safety and Health Administration (MSHA) mandates the use of a continuous personal dust monitor (CPDM), a battery-powered device that the miner wears on his or her belt to take continuous dust samples for designated occupations and designated areas (30 CFR § 70).

Among the safety hazards in an underground coal mine is the risk that a miner may become struck or pinned by a piece of mobile machinery such as a continuous mining machine or other mobile equipment. To address this hazard, MSHA requires that all continuous mining machines, except full-face machines, must be equipped with a proximity detection system (PDS) (30 CFR § 75.1732). A PDS consists of machine-mounted and miner-wearable components (MWCs) that communicate with low-frequency signals to determine the position of the miner relative to the machine and to issue warnings or automatically disable machine motion in order to prevent the machine from contacting the miner. The miner-wearable component of the PDS is typically worn by the miner on his or her belt. Since the PDM is also worn on the miner's belt, these two devices can be placed near each other.

Incidents of electromagnetic interference (EMI) of one model of CPDM, which we will refer to as the PDM, with the PDS in underground coal mines have been reported, and NIOSH researchers have verified through laboratory experiments that EMI is occurring. The EMI affects the readings of an MWC of the PDS in such a way that the calculated location of the miner becomes unreliable. This creates a serious safety concern since it can effectively render the PDS non-

✉ Jingcheng Li
JLi16@cdc.gov

[1] Pittsburgh Mining Research Division, National Institute for Occupational Safety and Health, 626 Cochrans Mill Road, Pittsburgh, PA 15236, USA

operational during the EMI incident. As a result of EMI, miners working near a machine can be in a risk position without knowing it. For the miner's safety, NIOSH researchers have conducted research into EMI mitigation strategies.

In an effort to mitigate the effects of this EMI, large shielding pouches and boxes were developed to enclose the entire PDM to reduce its magnetic emission. Research showed that the pouches and boxes reduced the emitted radiation, but they also disturbed the magnetic field, affecting the performance of the PDS [4–6].

In order to find a better solution, researchers from the NIOSH have turned their focus from external shielding of the entire PDM to internal shielding of individual PDM components. The research team identified the PDM air pump motor as one of the major sources of electromagnetic radiation within the PDM and selected this pump assembly for further tests. The research team conducted a series of tests on this pump and showed that a copper or aluminum foil enclosure can effectively reduce the magnetic emission from the motor by between 50 and 85% at 73 kHz, which is the operating frequency of one MSHA-approved PDS used in underground mines. With this shielding around the pump motor, the magnetic emission of the motor is reduced to well below the susceptibility threshold at which it could interfere with the PDS. While this result is promising, it should be noted that the air pump motor is only one of several components within the PDM that may cause EMI. An investigation of the other components within the PDM is currently underway. This study compares the shielding effects of copper, aluminum, and other cost-effective materials that could be used to shield the motor. The information provided in this paper can be used by PDM and other electronic device manufacturers to develop an EMI shielding strategy for internal device components; this could make mines safer by mitigating the problems of EMI and thereby maintaining the normal and safe performance of PDSs.

2 Method and Experimental Setup

NIOSH researchers have developed a test method to measure the shielding effectiveness of the enclosures that are particularly applicable to the air pump motor. Some standardized EMI measurement methods, such as RE101, were referenced and adapted in the development of the NIOSH test method [1, 2]. In addition, the method of determination of shielding effectiveness was also developed by referencing and adapting some standardized methods [3, 7]. In the experiment, the enclosure was made to directly touch the surfaces of the air pump motor assembly, which has an irregular shape.

The maxon A-max 303774 motor used to drive the air pump in the assembly is a 12-V DC brushed motor. This type of motor has a commutator with stationary carbon brushes sliding over it while it turns to rapidly switch armature current. This current switching can produce a significant electromagnetic emission.

A 12-V supply with a pulse-width modulation (PWM) mode is used to control the speed of the motor. These series output pulses can generate electrical noise over a wide spectrum range. In a PDM, the pulse width changes with changes in measurements from on-board temperature, humidity, and other sensors. To measure emission exclusively from the motor, the motor was removed from the PDM case and provided with a stabilized 12-V pulse supply while varying the frequency of the pulse. During testing, two diode snubbers remained connected to the motor terminals. A total of 12 pulse frequencies were selected, which included DC, 10 Hz, 20 Hz, 30 Hz, 40 Hz, 50 Hz, 100 Hz, 200 Hz, 500 Hz, 1000 Hz, 1500 Hz, and 2000 Hz. Figure 1 shows the block diagram of the experimental setup. Figure 2 demonstrates the wave form of a pulse supply voltage.

As shown in Fig. 1, the air pump motor was powered by the 12-V pulse supply via a 140.0-cm (55.12 in.) cable. An AL-RE101 antenna was used to measure the magnetic field emission of the motor at a distance of 7 cm (2.76 in.). This is the distance that is used by a standardized RE101 test [2]. The side of the motor to be measured was turned to face the center of the receiving antenna at 7 cm, and this practice was followed for each side of the motor. The antenna feeds the emission measurements from the motor to a Tektronix RSA5103A Real-Time Signal Analyzer via a 183.0-cm (72.0 in.) coaxial cable. The signal analyzer stores the raw measurement data in a unit of dBμV. The data were transferred to a computer to convert to magnetic flux density readings in dBpT. The standardized RE101 test uses dBμV as the basic measurement unit, and the manufacturer of a standardized RE101 receiving antenna provides conversion factors from dBμV to dBμT. These conversion factors are factory-determined and frequency-dependent.

Prior to the emission measurement of the motor, the emission of the pulse power supply unit was measured at a distance

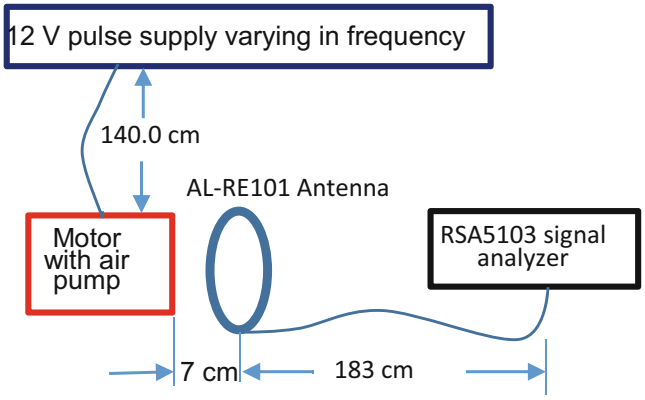

Fig. 1 Block diagram of the experimental setup for the PDM air pump motor

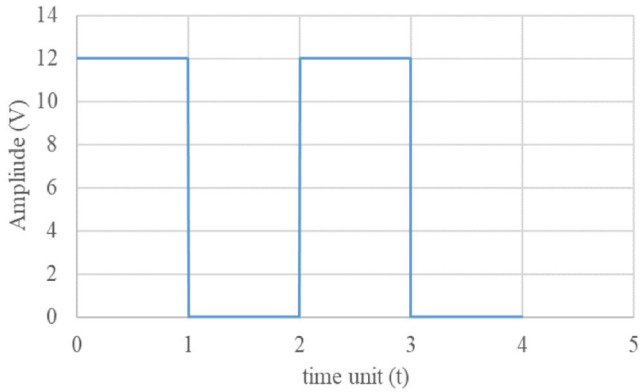

Fig. 2 Illustration of pulse supply voltage to the motor

of 140.0 cm. These measurements showed that the power supply unit would have a very insignificant influence on the emission measurements of the motor. The measurements also showed that the influence of the signal analyzer on the antenna was very insignificant. Furthermore, the measurements showed that the ambient electromagnetic noise was low.

Figure 3 shows the air pump motor assembly; the metallic cylinder in the photograph is the electric motor and the black plastic housing attached to the motor contains the air pump. The magnetic field emission measurements were made on six orthogonal sides of the air pump motor assembly. The sides of the motor were numbered as shown in Fig. 3. Figure 4 shows a picture of the motor with one side (side 3) sitting on the test platform with no shielding materials applied. The air pump has a rubber air tube connected with an air filter at the opposite end of the tube.

The AL-RE101 antenna has a usable frequency range of 10 Hz to 1 MHz. In this experiment, the measurements of the emitted magnetic field from the motor were set in a frequency band from 10 to 150 kHz, which covers the operating frequencies used by all of the current commercial PDSs. Any unintended magnetic field emissions from the motor in this

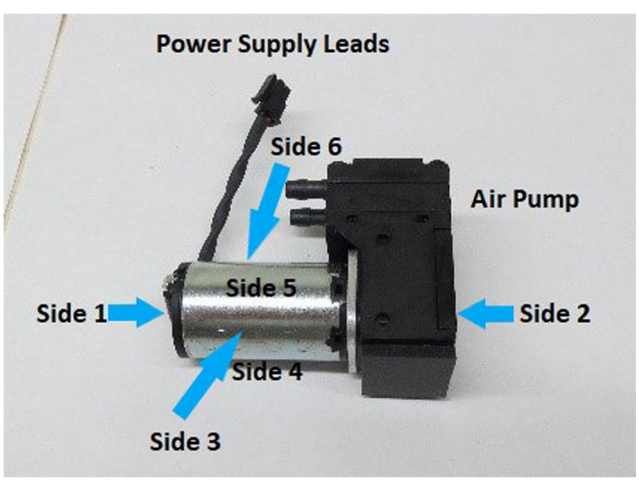

Fig. 3 Assembly of air pump and motor (side 4 on the bottom of the motor)

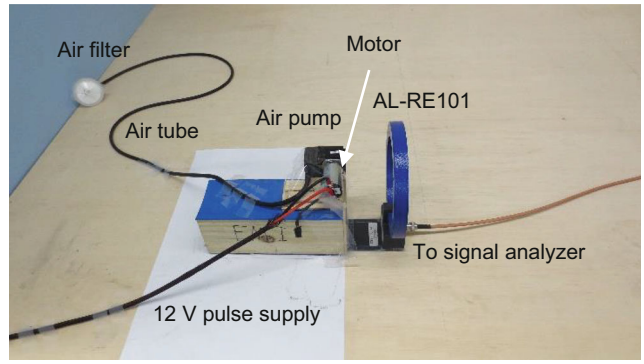

Fig. 4 Motor with its one side (side 3) sitting on test platform

frequency band that could cause an interference with the proximity detection systems can then be identified.

3 Test Results

The magnetic field emission measurement on the motor began with no shielding material applied. The emissions from the six sides of the motor were measured individually and used as the baseline of the motor emission. The baseline emission measurement from each side was later compared with the emission measurement of the corresponding side of the motor with different shielding materials applied. The shielding effect of each of the materials was then identified by the emission differences.

The tight packing of the components surrounding the motor assembly inside of a PDM leaves little room for a shielding enclosure for the motor. In addition, the PDM has a weight restriction. Some light, thin, and flexible materials were, therefore, allowed to be used to shield the motor assembly. The shielding materials and their thicknesses used in the experiment were aluminum foil of 0.0254 mm (0.001 in.), aluminum foil of 0.0508 mm (0.002 in.), copper foil of 0.016256 mm (0.00064 in.), copper mesh of 0.1143 mm (0.0045 in.) diameter wire and 0.1397 mm

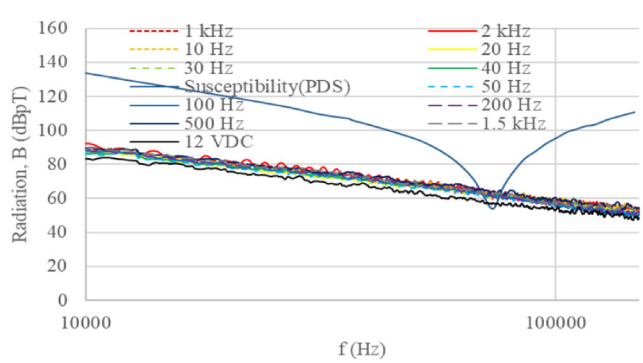

Fig. 5 Comparing magnetic field emission from side 3 of the motor having no shielding to the susceptibility of a PDS

(0.0055 in.) opening, graphene sheet of 0.254 mm (0.01 in.), stainless steel mesh of 0.09906 mm (0.0039 in.) diameter wire and 0.09906 mm (0.0039 in.) opening, and silver-graphene epoxy.

Figure 5 shows the magnetic field emission measurements from side 3 of the motor with no shielding material applied, referring to Fig. 4 for the experimental setup. In addition to the emission spectra, from 10 to 150 kHz, of the motor with 12 supply voltages in different pulse frequencies, a susceptibility curve, labeled as susceptibility (PDS), of a PDS measured in NIOSH's previous research [4] is also given in the figure for the purpose of identifying potential EMI from motor emissions. Any portion of an emission curve for the motor found to be above the susceptibility curve suggests that there is a high potential for interference to occur because of the stronger energy of the emitted magnetic field of the motor compared with the susceptibility of the PDS. The emission curves of the motor produced from the 12 supplied pulse voltages, as shown in Fig. 5, have a high potential to cause an interference around 73 kHz because these emission curves all pass above the PDS susceptibility frequency around 73 kHz. Seventy-three kilohertz is the operation frequency of the PDS used in this experiment. This is the basic reason that the susceptibility curve (as shown in Fig. 5) of an MWC of the PDS shows the lowest value at 73 kHz, and EMIs would mostly occur around this frequency, since interference can occur there at much lower energy levels than at other frequencies. For this reason, the emission of the motor at 73 kHz is particularly interesting to NIOSH researchers, and the shielding effectiveness analysis mostly focused on this frequency. Figure 5 provides a systematical method to identify whether the emissions of the motor can potentially cause EMI with an MWC of a PDS. This method will be used in the following discussion.

As shown in Fig. 5, the motor showed a strong emission from 10 to 150 kHz even with a 12-V DC supply. This is because of the rapidly switched current for armature on commutator. A pulsed 12-V supply would create additional emissions.

The measurements showed that all six sides had very similar emission patterns to that given in Fig. 5 with, however, different amplitudes. A lower emission was found from two ends (sides 1 and 2 as shown in Fig. 3) of the motor, and the emission from side 2 was the only one showing its curves below the susceptibility of the MWC of the PSD suggesting that the emission of side 2 would not cause EMI. The remaining sides were all found have much higher emissions, although with slightly different amplitudes. For this reason, the emission measurements from side 3 are used to typify the emission of the motor in the following discussions.

Figure 6 shows the experimental setup for the emitted magnetic field measurement of side 3 of the motor shielded completely with one layer of 0.0508-mm aluminum foil. The shielding layer was tightly wrapped on the motor with the adhesive insulation tape to hold and form an enclosure from outside. The shielding was also extended around the immediate leads of the motor. No electrical ground connection was made between the shielding enclosure and the motor. Figure 7 shows the magnetic field emission measurements from side 3 of the shielded motor. Comparing the emission measurements of the side 3 with the baseline, shown in Fig. 5, one could find that the aluminum foil brought all emission curves downward. A calculation from the computer program developed in this study shows that the shielding enclosure attenuates the magnetic energy emission by 71.37% on average at 73 kHz.

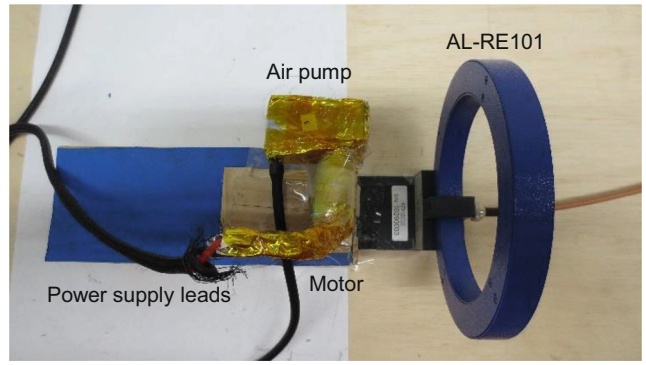

Fig. 6 Motor shielded with aluminum foil of 0.0508-mm (0.002 in.) thickness

Figure 8 shows the magnetic field emission measurements from side 3 of the motor shielded with one layer of copper mesh with a wire diameter of 0.1143 mm (0.0045 in.) and an opening of 0.1397 mm (0.0055 in.). The motor was shielded in the same manner as that with the aluminum enclosure shown in Fig. 6.

As shown in Fig. 8, all of the emission curves of side 3 of the motor were brought down by the copper mesh enclosure further than the aluminum foil enclosure. As a result, the emission no longer has a potential to interfere with the PDS. A calculation from the computer program developed in this study shows that the copper mesh enclosure attenuates the

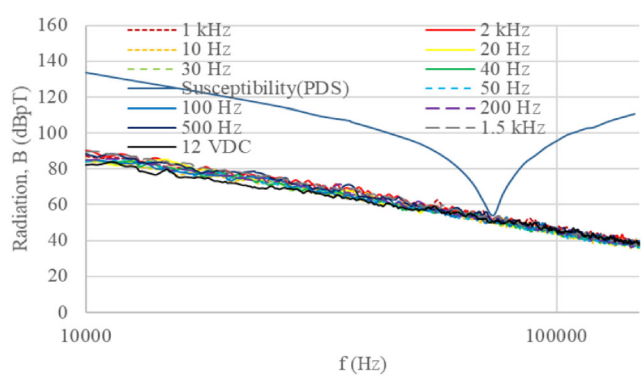

Fig. 7 Magnetic field emissions from side 3 of the motor shielded with one layer of aluminum foil of 0.0508-mm or 0.002-in. thickness

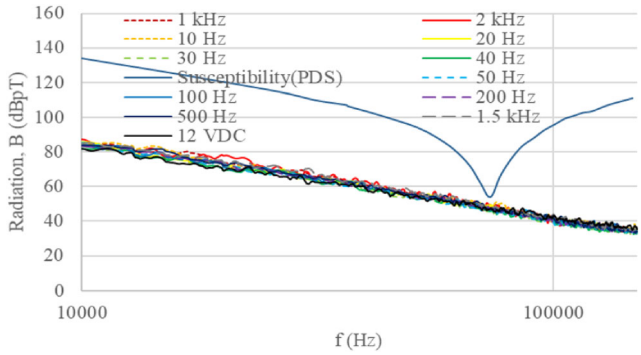

Fig. 8 Magnetic field emission from side 3 of the motor shielded with an enclosure of one layer of copper mesh with wire diameter of 0.1143 mm (0.0045 in.) and opening of 0.1397 mm (0.0055 in.)

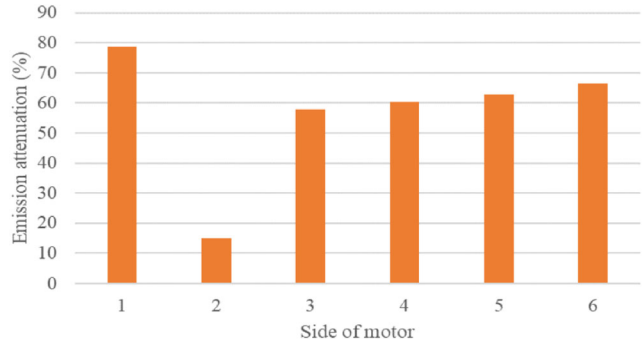

Fig. 10 Comparison of the average emission attenuations of six sides of the motor shielded with copper foil of 0.016256-mm (0.00064 in.) thickness at 73 kHz

emission from side 3 of the motor by 84.92% on average at 73 kHz.

With the same shielding manner, we measured the emissions from side 3 of the motor with each of the shielding materials. Figure 9 shows the average emission attenuations of those different shielding materials and material thicknesses at 73 kHz on the emission from side 3 of the motor. In Fig. 9, Al .001" stands for aluminum foil with 0.001-in. thickness, Al .002" for aluminum foil with 0.002-in. thickness, Cu .00064 for copper foil with 0.00064-in. thickness, Ag-graphene for silver-graphene epoxy, and Cu mesh for copper mesh. Copper and aluminum clearly show a higher shielding effect than the other materials and were more effective with greater thickness.

The magnetic field emission from each of the sides of the motor was measured in the same manner with each of the shielding materials. The measurements show that the emission attenuations were different from different sides, even with the same shielding material. For example, Fig. 10 shows the average emission attenuation of each of the sides of the motor shielded with copper foil at 73 kHz. As it can be seen, the copper foil did not equally attenuate the magnetic emission on all of sides of the motor. Note that the measurements also show that the magnetic field emission strength from each side of the motor with no shielding material applied was also largely different from each other. Side 2 had the lowest no-shielding emission, which also had the lowest emission attenuation as shown in Fig. 10.

Figure 11 shows the average emission attenuations with different shielding materials on all of the sides of the motor at 73 kHz. Similar to side 3, copper and aluminum show a higher effectiveness at attenuating the emission of the motor and more effective with greater thickness. The thicker aluminum enclosure was shown to have a higher attenuation percentage value than the thinner one. The thicker copper enclosure also shows a higher attenuation percentage value than the thinner one.

4 Discussion

As shown in Section 3, the highest emission was found from the longitude side surfaces of the motor. This suggests that reducing the emission from these sides of the motor can reduce overall emission of the motor. If the manufacturer wishes to design a motor with a low emission, focusing on emission reduction of side surfaces of the motor would be most effective. This also suggests that re-orientating the motor in a PDM

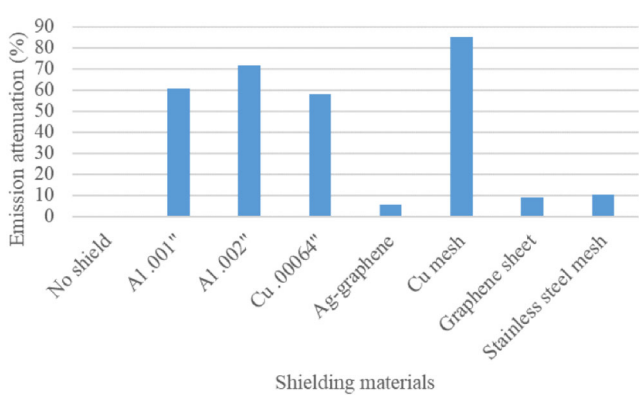

Fig. 9 Average emission attenuations on side 3 of the motor with different shielding materials

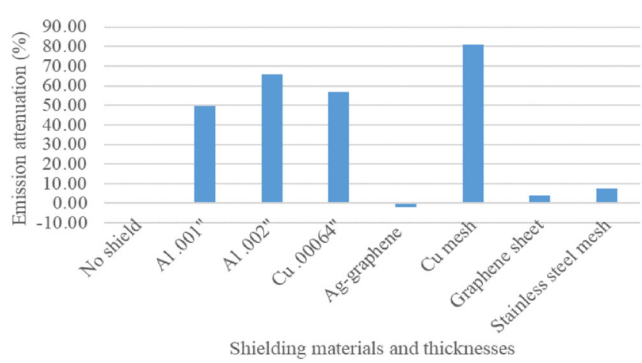

Fig. 11 Comparison of the average emission attenuations by the shielding materials and their thicknesses on all of six sides of the motor at 73 kHz

in such a way that its lowest emitting side faces an MWC of a PDS can potentially reduce a chance for EMI.

As shown in Fig. 11, aluminum and copper show a higher attenuation rate on the emitted magnetic energy of the motor at 73 kHz than any of the other materials tested. The figure also shows that an enclosure with a thicker layer of shielding has a higher emission attenuation rate than that with a thinner one. This suggests that the shielding material and its thickness are important factors to consider for a shielding enclosure design for the motor.

Measurements show that the shielding effectiveness is different from one side of the enclosure to another. This suggests that each of the sides of the enclosure not only shields part of the magnetic energy from that side of the motor but also reflects part of the energy back, resulting in a redistribution of magnetic energy within the enclosure. This could cause the emission from another side to slightly increase rather than decrease as it showed in the case of silver-graphene epoxy. As shown in Fig. 11, a magnetic emission increase from one of the enclosures causes the average emission to increase with silver-graphene. Further study may be needed to understand this phenomenon in order to not only develop better shielding enclosures but also to prevent the motor's electrical characteristics from potentially being altered by the intensified magnetic energy within the enclosure caused by the shielding enclosures.

A complete coverage over the motor with a shielding enclosure is required in order to achieve a high effectiveness of shielding. Our measurements show that an intensified magnetic energy could be measured from even a small opening on a shielding enclosure. This suggests that the magnetic energy produced from the motor can be redirected by the internal surfaces of the shielding enclosure and released from a small opening of the enclosure. This also suggests that an enclosure can be designed with an opening on it to release the magnetic energy from it in a direction which causes no interference to other systems.

It was a very challenging task to maintain consistency among the different shielding materials used to manually wrap the motor. To minimize any possible negative impact on the emission measurement due to wrapping inconsistencies, a dedicated technician was appointed to perform the job, a conductive tape was used to tightly hold the wrappings to the surfaces of the motor, and photos were taken of the enclosures made from different materials. Researchers consistently examined the measurements and repeated the work whenever any doubtful data was found. It was found that a small opening on an enclosure could make a notable difference in the measured emission. Whenever this happened, the wrapping was repeated. All the enclosures used in the experiments were saved since they could serve as samples when enclosures needed to be copied to repeat a test.

In a separate experiment, researchers measured the magnetic field emission from the motor with lower DC supply voltages than its normal value of 12 VDC and found that a lower emission was always associated with a lower voltage. The measurements were not presented in this paper because those lower voltages were not considered to be normal. However, it shows that a supply voltage is indeed a factor that influences the strength of the emitted magnetic field of the motor.

5 Limitations

The quantitative analysis of the effectiveness of the shielding materials used in this research was based on the electromagnetic emission measurements from only one air pump motor of PDM at one laboratory condition. Additional measurements need to be made from additional motors under different testing conditions in order to determine the variation of electromagnetic emissions among motors under various operating conditions. The data can help with cost-effective selections for shielding materials and choice for shielding enclosure design, which cover a range of the motors.

6 Conclusions

NIOSH researchers conducted this research with the intention to help develop EMI mitigation strategies for a continuous personal dust monitor, which was found to electromagnetically interfere with magnetic proximity detection system used in underground coal mines. Tests showed that air pump motor in the PDM was one of the strongest electromagnetic sources. To help further possible enclosure designs to shield the air pump motor, this paper presents the test results of some selected cost-effective shielding materials for the motor for the purpose of identifying the effectiveness of these materials on magnetic field shielding for the motor. The measurements show that the strongest emission was from the longitude side surfaces of motor. The measurements also show that aluminum and copper can shield the magnetic energy emission of the motor more effectively than any other tested materials. The measurements, in addition, show that the thicker a shielding enclosure is, the more effective the shielding. The results provide quantitative measurement data that can assist in the development of effective EMI shielding strategies for the air pump motor and also for other electronic systems used in underground mines to increase electromagnetic compatibility in mines and improve safety for miners.

Acknowledgments The authors sincerely thank Mr. Donald Tuchman, Industrial Hygienist of NIOSH, for his support of this work, his comments and data reviewing in the process of this work, and his efforts to provide us with a PDM test unit and other PDM components. The authors also want to express their thanks to Thermo Fisher Scientific for the samples of air pump motor units provided for this work. In addition, we want to thank the Dust, Ventilation, and Toxic Substances Branch of the Pittsburgh Mining Research Division of NIOSH for providing support in this work.

Compliance with Ethical Standards

Disclaimer The findings and conclusions in this report are those of the authors and do not necessarily represent the official position of the National Institute for Occupational Safety and Health, Centers for Disease Control and Prevention. Mention of any company or product does not constitute endorsement by NIOSH and CDC.

Conflict of Interest The authors declare that they have no conflict of interest.

References

1. Eckert J (1988) Commercial EMC standards of the United States, vol 9. Interference Control Technology, Inc, pp J9–J22
2. MIL-STD-461F, pp 91–94 10, December 2007. https://snebulos.mit.edu/projects/reference/MIL-STD/MIL-STD-461F.pdf. Accessed 19 July 2019
3. Montrose M, Nakauchi E (2004) Testing for EMC compliance approaches and techniques. IEEE Press, Wiley-Interscience, Wiley, Hoboken, pp 330–333
4. Noll J, Matetic RJ, Li J, Zhou C, DuCarme J; Reyes M, Srednicki J (2017) Electromagnetic interference with proximity detection systems. Published in proceedings of Annual Conference of Society of Mining, Metallurgy and Exploration, Denver CO, Feb 19–22
5. Noll J, Li J, DeGennaro C, Zhou C, Srednicki J (2018) Evaluation of different shielding materials for reducing electromagnetic interference of the ersonal dust monitor. Published in proceedings of Annual Conference of Society of Mining, Metallurgy and Exploration, Minneapolis MN, Feb 25–28, 2018
6. Noll J, Matetic RJ, Li J, Zhou C, DuCarme J, Reyes M, Srednicki J (2018) Electromagnetic interference from personal dust monitors and other electronic devices with proximity detection systems. J Min Eng 70(5):61–68
7. Ott H (2009) Shielding. In: Electromagnetic compatibility engineering. Wiley, Hoboken, pp 238–245